Materials Research Letters

ISSN: (Print) 2166-3831 (Online) Journal homepage: https://www.tandfonline.com/loi/tmrl20

Grain-subdivision-dominated microstructure evolution in shear bands at high rates

Xiaolong Ma, Dexin Zhao, Shwetabh Yadav, Dinakar Sagapuram & Kelvin Y. Xie

To cite this article: Xiaolong Ma, Dexin Zhao, Shwetabh Yadav, Dinakar Sagapuram & Kelvin Y. Xie (2020) Grain-subdivision-dominated microstructure evolution in shear bands at high rates, Materials Research Letters, 8:9, 328-334, DOI: 10.1080/21663831.2020.1759155

To link to this article: https://doi.org/10.1080/21663831.2020.1759155

MATER. RES. LETT.
2020, VOL. 8, NO. 9, 328–334
https://doi.org/10.1080/21663831.2020.1759155

MATERIALS RESEARCH LETTERS
Taylor & Francis
Taylor & Francis Group

ORIGINAL REPORT

OPEN ACCESS Check for updates

Grain-subdivision-dominated microstructure evolution in shear bands at high rates

Xiaolong Ma [a], Dexin Zhao[a], Shwetabh Yadav[b], Dinakar Sagapuram[a,b] and Kelvin Y. Xie[a]

[a]Department of Materials Science and Engineering, Texas A&M University, College Station, TX, USA; [b]Department of Industrial & Systems Engineering, Texas A&M University, College Station, TX, USA

ABSTRACT
Shear banding is an important deformation and failure mechanism in metallic systems, especially at high-rate straining. Dynamic recrystallization was often reported to account for the refined microstructure of shear bands but rarely confirmed using direct quantitative measurement. Here, we employ quantitative precession electron diffraction analysis to uncover shear band microstructure in pure titanium. The results reveal that the microstructure is dominated by early stages of grain subdivision process. Dynamic recrystallization is not as prevalent as perceived conventionally. Our results offer key insights into understanding shear banding and highlight the need for quantitative analyses of shear band microstructure.

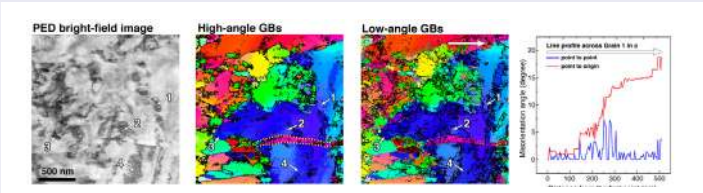

IMPACT STATEMENT
A critical quantitative assessment of shear band microstructures is made using precession beam diffraction imaging. Specifically, grain subdivision, as opposed to dynamic recrystallization, drives the shear band microstructure evolution.

ARTICLE HISTORY
Received 11 December 2019

KEYWORDS
Shear banding; dynamic recrystallization; precession electron diffraction; grain subdivision

1. Introduction

Shear banding, a type of inhomogeneous plastic flow mode, is considered as one of the most important failure mechanisms in high strain rate deformation of polycrystalline metals [1–3]. Shear banding represents localization of large plastic strains (shear strains up to 10^2) in thin microscopic bands even when the imposed (macroscopic) deformation state is homogeneous [4]. Shear banding is typically promoted by low thermal conductivity of the material and high strain rates ($> 10^3 s^{-1}$), factors that promote adiabatic deformation conditions [5]. At a continuum level, the onset of plastic instability, causing the transition from homogeneous to shear band flow, is associated with the maximum on the stress–strain curve, i.e., the point where flow stress softening balances the hardening [6]. While strain and/or strain rate hardening contribute to the flow stress increase, temperature rise (due to plastic work) has been considered as the primary mechanism that leads to softening for decades [1,6]. In the last few decades, the thermal softening mechanism appears to be supported by two major sets of experimental observations. The first is the accompanying local temperature rise in the shear band [7–9]. The second is the widely reported dynamic recrystallization (DRX) in shear bands [10–23]. Interestingly, recent studies, involving *in situ* measurements of shear bands, however indicate minimal role of temperature rise, at least, in the shear band initiation [24]. This finding also inspires us to

CONTACT Dinakar Sagapuram dinakar@tamu.edu Department of Materials Science and Engineering, Texas A&M University, College Station, TX 77843, USA; Department of Industrial & Systems Engineering, Texas A&M University, College Station, TX 77843, USA; Kelvin Y. Xie kelvin_xie@tamu.edu Department of Materials Science and Engineering, Texas A&M University, College Station, TX 77843, USA

Supplemental data for this article can be accessed here. https://doi.org/10.1080/21663831.2020.1759155

reevaluate the shear band microstructure in early investigations, particularly to quantify the level of DRX and other characteristics in the microstructure.

The basic premise of DRX, either continuous or discontinuous, is the formation of new grains that are strain/dislocation free and bounded by high-angle grain boundaries (HAGBs) driven by the stored energy of deformation [25,26]. Traditionally, the occurrence of DRX has been often reported by post-mortem observations of ultrafine or nanoscale grains within the shear band using conventional transmission electron microscopy (TEM) techniques [12,16,18,22,23]. It is important to note that these grains have been often described as having low dislocation density and high angle grain boundaries (indicators of recrystallization), purely based on the diffraction contrast. DRX has been rarely confirmed using direct quantitative measurements of grain boundary misorientations and their overall statistics. It is well known that the diffraction contrast in TEM is highly sensitive to the misorientation: a few degrees of crystal misorientation could result in dramatic changes in contrast [27]. Therefore, conventional bright-field and dark-field imaging techniques by themselves cannot distinguish between the subgrains separated by low angle grain boundaries (LAGBs) from newly recrystallized grains that are typically characterized by HAGBs.

In light of the above challenge, we employed precession electron diffraction (PED) in TEM to quantitatively map the shear band microstructure in commercially pure Ti in terms of crystal orientation and grain boundary misorientation. PED, while similar to electron backscatter diffraction (EBSD), offers higher spatial resolution ($\sim$1 nm) needed for shear band analysis [28]. We show that microstructure evolution within a band is characterized by an early stage of the grain subdivision process, where LAGBs dominate the microstructure. In particular, we show that DRX is not as prevalent as generally perceived based on conventional TEM analyses. The overall microstructure bears a strong resemblance to those resulting from severe plastic deformation at ambient temperatures. Our results provide key quantitative information pertaining to microstructure evolution within shear bands. The direct observations from this work are also of value to computational models aimed at predicting the initiation and propagation of shear bands.

2. Materials and methods

Commercially pure (CP) Ti (grade 2) was used in this study. The material was received in a plate form with an annealed condition (215 HV) and an average grain size of $\sim 100\mu$m (see Figure S1). Two-dimensional plane strain cutting was used as an experimental framework to impose controlled simple shear, which allows the study of single shear bands without interfering effects from other bands [29]. A thin layer of material ($t_0 = 125\mu$m) was removed from a workpiece surface in the form of a 'chip' via simple shear imposed by a sharp wedge-shaped tool at a velocity (V_0) of 10 m/s (Figure S2) [4,29]. The chip thus produced was characterized by periodic shear band structures (Figure S2). Details of this technique can be found in our earlier reports [4,30].

The material microstructural characteristics in and around shear bands were studied using EBSD and TEM. The specimens were firstly mechanically ground and then electrochemically polished to perforation using an electrolyte of 5% perchloric acid, 35% butanol, and 60% methanol at -40°C. A Tescan FERA-3 scanning electron microscope (SEM) was used to obtain EBSD inverse pole figure (IPF) maps (0.5μm step size). Conventional bright-field micrographs and diffraction patterns were obtained using an FEI Tecnai G2 F20 TEM operated at 200 kV. The PED experiments were carried out in a Titan TEM operated at 300 kV equipped with a NanoMEGAS ASTAR system [31]. The orientation mapping was done at a procession-beam angle of 0.6° and a step size of 4 nm.

3. Results and discussion

Figure 1(a) shows an SEM image of the shear banded sample, where the light striations on the chip are the deformed pre-inscribed markers. The sharp displacement of markers across the shear band is indicative of the intense localized flow around the band. The labeled markers (1–4) illustrate the large and uniform shear displacement ($\sim 100\,\mu$m) along the shear band. Note that the displacements across the band result purely from highly localized shear over a thin interface (shear band), and not from fracture, as clearly seen from the chip microstructure in Figure 1(b). Quantitative strain calculations by tracking local changes in the curvature of markers have revealed large shear strains of ~ 40 at shear band center [4]. The local strain rate experienced by the band is expected to be in the $10^6 s^{-1}$ range [29].

The global microstructural details around the band, resolved using EBSD IPF maps (taken from the flow-transverse plane in Figure 1, i.e., top-view of the chip), are shown in Figure 2(a). Regions outside shear bands are comprised of large grains with an average size of $\sim 10\mu$m and seem to have been only slightly deformed. Some {10–12} extension twins were also observed in these regions. In contrast, microstructure within shear bands could not be resolved using EBSD and appeared as two non-indexed vertical bands in Figure 2(a). This

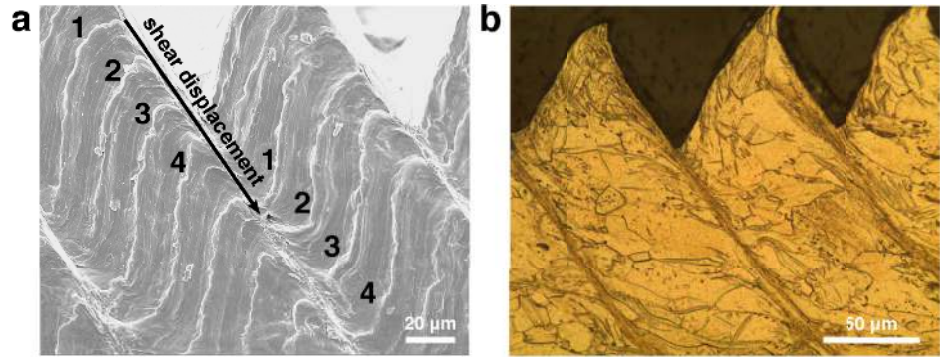

Figure 1. (a) SEM micrograph showing the morphology of micromarkers in a shear-banded chip of CP Ti cut with $V_0 = 10$ m/s. The black arrow indicates the shear displacement caused by shear banding. (b) Optical micrograph of shear bands in the chip.

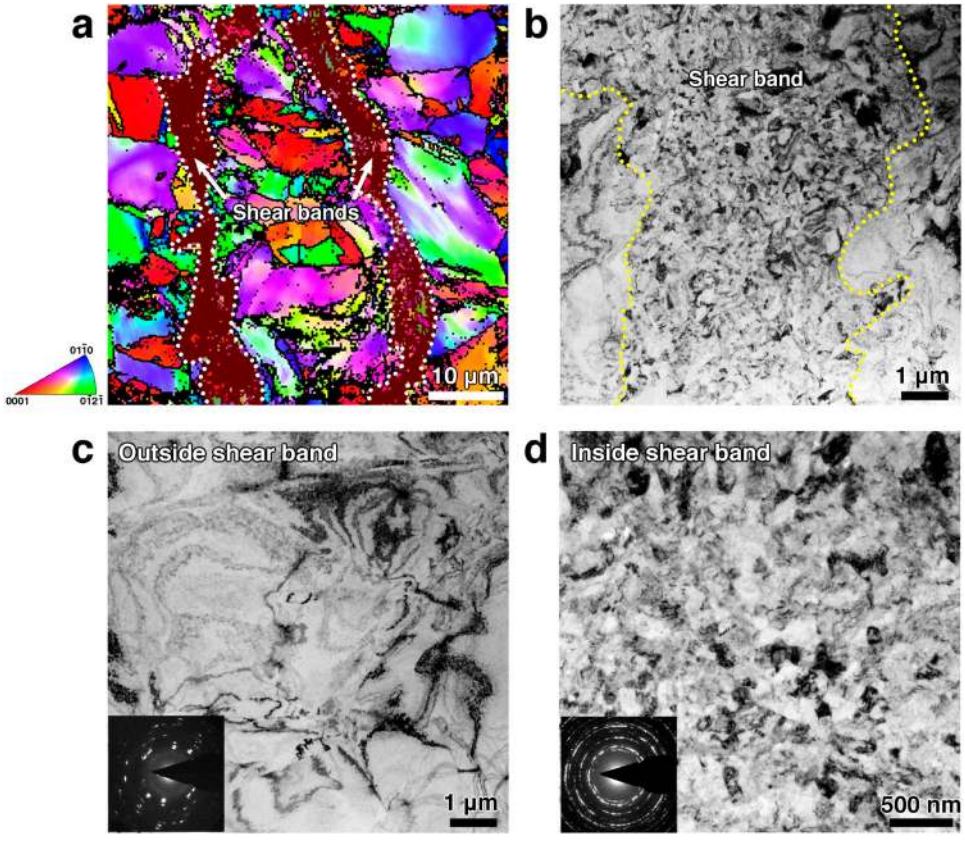

Figure 2. (a) Top-view EBSD IPF mapping of the machined strip. The shaded, narrow regions correspond to the shear bands. (b) A representative bright-field TEM micrograph covering a shear band and its neighborhood. The shear band boundaries are marked with dotted lines. (c) A bright-field TEM micrograph outside shear band and its corresponding SAED. (d) A magnified bright-field TEM micrograph in the center of a shear band and its corresponding SAED, showing the dramatically refined microstructure.

is a consequence of the high strains and highly refined microstructure within the band. Local microstructural information at a higher resolution was obtained using bright-field TEM, as shown in Figure 2(b–d). Figure 2(b) shows a representative shear band and its neighboring less-deformed regions. The shear band boundaries are highlighted by dotted lines for reference. The shear band width was about 3–4 μm, consistent with our previous estimates of the width based on strain measurements [4]. The coarse-grained regions outside the band exhibit local bending contours, typical of grains with some straining (Figure 2(c)). In comparison, within the shear band (Figure 2(d)), the microstructure is highly refined, further substantiated by a ring-like diffraction pattern (see inset). The fine-grained shear band microstructure seen here bears a strong resemblance to other reports of shear band microstructures in Ti and its alloys, many of which have been interpreted in terms of DRX [10,12,16].

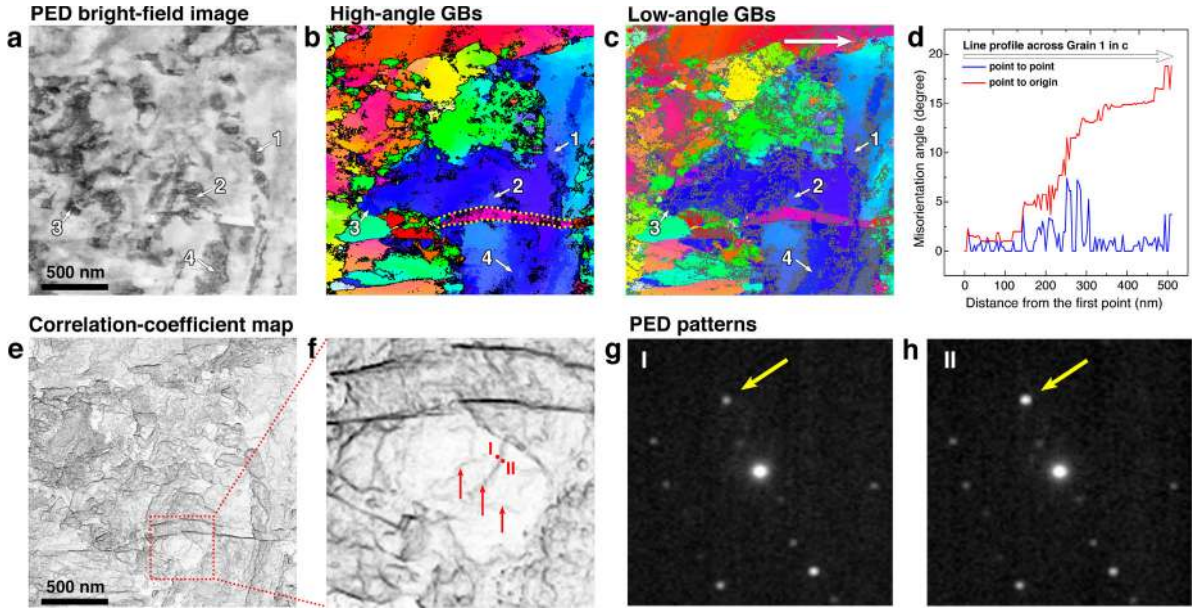

Figure 3. PED characterization of the microstructure in the center of shear band. (a) PED bright-field image. (b) HAGB (black) and (c) LAGB (gray) on top of the orientation map of the region of interest. The yellow dotted lines highlight a contraction twin. The numbered grains (1–4) in (a)–(c) are example of subgrains that are fully or partially bounded by LAGBs. (d) The misorientation line profile corresponds to the arrow in (c). (e) The correlative coefficient map of (a). (f) Zoomed-in view of the highlighted box in (d). The arrows indicate the presence of dislocations. (g) and (h) The PED patterns correspond to the labeled spots I and II in (e).

To achieve a more quantitative analysis of shear band beyond the limits of conventional TEM imaging, we collected PED data in the band center, as summarized in Figure 3. Figure 3(a) shows a PED bright-field image from the shear band center. This image resembles the conventional bright-field image in Figure 2(d). A conventional interpretation of the random bright/dark contrasts with feature sizes of tens or hundreds of nanometers would have been to assume that the region of interest has been 'recrystallized' into ultrafine grains. However, the IPF maps in Figures 3(b,c) show that these ultrafine grains with distinct diffraction contrast actually exhibit very similar crystal orientation, with most of them separated by the LAGBs (2–15°). This suggests that these features are likely a result of the parent grain being refined/partitioned into numerous subgrains under the influence of severe mechanical deformation. For example, a relatively large blue grain in the lower-right corner in Figure 3(c) contains considerable subgrains separated mainly by LAGBs. Subgrains, such as the numbered grains 1–4, could be potentially, and have been in the past, incorrectly identified as the recrystallized grains based on conventional bright- or dark-field images. A brief remark regarding how LAGBs can give rise to arcs or rings in the diffraction pattern (Figure 2(d)), which are usually used as indicators for DRX, is perhaps in order. Although the misorientations across each LAGB are small, their accumulation over a distance can result in considerably large misorientation values. This is illustrated in Figure 3(d), where the misorientation data along a line scan spanning multiple subgrain boundaries (top white arrow in Figure 3(c)) is shown. The point-to-point misorientation (represented by blue curve, Figure 3(d)) is small, but the point-to-origin plot (red curve) shows an accumulative misorientation up to $\sim 20°$.

Moreover, Figure 3(e) presents a visual representation of subgrains and their boundaries in the form of a correlation-coefficient map generated by weighting the similarities between the neighboring PED diffraction patterns. Here, darker lines or regions highlight the areas where neighboring diffraction patterns are most dissimilar, while brighter regions correspond to those with similar diffraction patterns. This representation enables the mapping of misorientations even less than 2°, and thus offers a powerful tool to visualize subgrain boundaries and dislocations arrays/bundles within. As an example, a zoomed-in view of a subgrain is shown in Figure 3(f), where gray lines within the subgrain interior (marked with red arrows) likely correspond to dislocations. This is further illustrated in Figure 3(g and h) which show the diffraction patterns from two locations (I and II) lying on either side of the dislocation line. The relative difference in the diffraction spot intensities at these locations (yellow arrows) is indicative of slight misorientation across the dislocation line in between. As seen from Figure 3(e), the correlation coefficient map reveals substantial levels

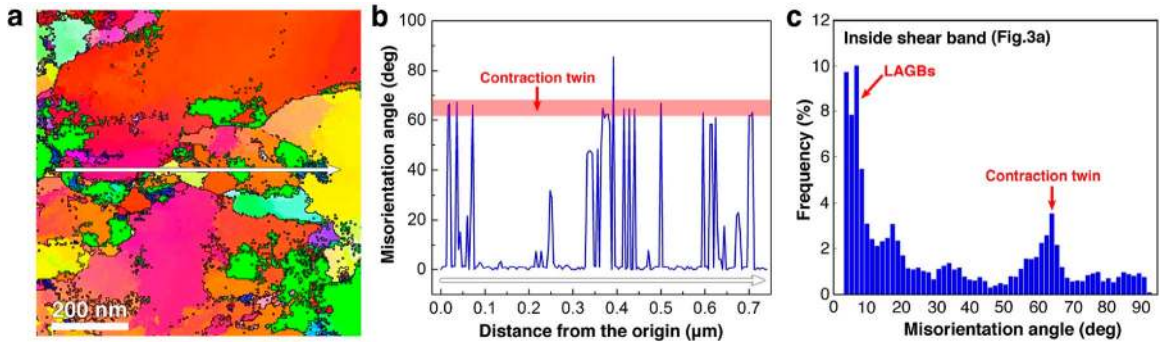

Figure 4. (a) A cropped PED map from Figure 3(b). (b) The misorientation line profile corresponding to the white arrow in (a). The shaded region highlights the contraction twin misorientation levels (65 ± 3°). (c) Misorientation angle distribution of inside-shear-band region in Fig.3a.

of dislocation structures within almost every single subgrain, even though these subgrains may appear 'pristine' or 'dislocation-free' in regular bright-field images. The fact that the subgrains are not defect-free lends further support that microstructure refinement within the band is not a result of DRX, but due to progressive breaking down of original grains into subgrains. That is, the underlying mechanism of microstructure evolution is that of grain subdivision, as is typical of severe plastic deformation processes [32,33].

Although LAGBs constitute the majority of observed boundaries, the PED scans over a shear band region also revealed some existence of HAGBs. Figure 4(a) is a ~ 700 nm x 700 nm view of a local region inside the band. The misorientation line profile in Figure 4(b) shows periodic grain boundaries with misorientation angles of 65 ± 3°, which coincidentally is the {1-212} contraction twin boundary character in Ti. The overall misorientation angle statistics across the entire shear band region (3 um x 3 um), shown in Figure 4(c), also reveals a prominent peak at ~65° corresponding to the contraction twins. However, note that the LAGBs (less than 15°) still constitute the majority, ~2/3rds. Contraction twins are not observed in the counterpart analysis of the regions outside the band (Figure S3). It is quite likely that contraction twinning has occurred during the initial stages of band formation, leaving debris of a number of HAGBs, since the planar characteristics of the twin boundaries were no longer preserved within the band (due to intense straining). It should be clear that without the quantitative misorientation data, as in conventional bright-field TEM [11,34], it would be challenging to delineate the high-angle twin boundaries from other LAGBs.

Taken as a whole, the quantitative PED results provide new insights into shear band microstructure evolution. As noted earlier, the shear band microstructure has been conventionally interpreted in terms of uniformly-distributed ultrafine grains resulting from DRX, often based on conventional bright-field TEM analysis. Here, using quantitative grain boundary misorientation statistics, we show that shear band microstructure is predominantly (~2/3rd) characterized by LAGBs with a misorientation angle less than 15°. DRX does not prevail the microstructure. The limited DRX here is of continuous type from a kinetics standpoint (briefly discussed in the *Supplementary Material*). More importantly, this together with other secondary observations pertaining to dislocation activity within subgrains (Figure 3(f–h)) and traces of deformation twinning (Figure 4) suggests that the mechanism underlying microstructural changes within the band can be represented as a grain subdivision process, as well documented in the past from the standpoint of severe plastic deformation processing [32,33]. In this process, initial (original) crystals are subdivided by the geometrically necessary boundaries (e.g. twin boundaries or part of dislocation slips) and incidental dislocation boundaries (dislocation cells and bundles) [34], where the misorientation angle across the geometrically necessary boundaries monotonically increases with the plastic strain later. The ultrafine LAGB structure seen inside the band therefore represents the early phase of the grain subdivision process, where HAGBs are not well developed yet in general. It is important to note that this grain subdivision process can take place even at ambient temperatures purely due to mechanical deformation [33,35], without thermal contributions. This further suggests that conventional thermally-driven DRX is not a prerequisite for shear banding.

Before proceeding to the conclusion, it should be noted that the final shear band microstructure critically depends on the local thermomechanical history experienced by the band during its initiation and growth. While the shear band microstructure studied here is representative of bands formed under high strain/strain rate conditions, it is certainly not universal. The focus here has been on highlighting the unique advantages

of quantitative PED method in shear band studies and in avoiding certain pitfalls associated with inferring microstructure evolution or softening mechanisms based on conventional TEM observations.

4. Conclusion

In summary, advanced precession electron diffraction TEM technique is used to quantitatively study the microstructure of shear bands produced in CP Ti under high rate deformation. These results reveal that a mechanically-driven grain subdivision process governs the microstructure evolution. DRX is clearly not as prevalent as perceived by conventional TEM. This work also highlights the need for quantitative high-resolution imaging techniques to reexamine shear band microstructures and associated softening mechanisms.

Acknowledgements

Dr. Kelvin Y. Xie acknowledges the start-up grant from the Department of Materials Science and Engineering at the Texas A&M University.

Disclosure statement

No potential conflict of interest was reported by the author(s).

Funding

This work was supported by Texas A and M Engineering Experiment Station, Texas A and M University.

ORCID

Xiaolong Ma http://orcid.org/0000-0003-1392-2787

References

[1] Antolovich SD, Armstrong RW. Plastic strain localization in metals: origins and consequences. Prog Mater Sci. 2014;59:1–160.
[2] Wright TW. Shear band susceptibility: work hardening materials. Int J Plast. 1992;8:583–602.
[3] Rittel D, Osovski S. Dynamic failure by adiabatic shear banding. Int J Fract. 2010;162:177–185.
[4] Sagapuram D, Viswanathan K, Trumble KP, et al. A common mechanism for evolution of single shear bands in large-strain deformation of metals. Philos Mag. 2018;98:3267–3299.
[5] Dodd B, Bai Y. Bai Y, editors. Adiabatic shear localization: frontiers and advances. 2nd ed. Amsterdam. Boston (MA): Elsevier; 2012.
[6] Zener C, Hollomon JH. Effect of strain rate upon plastic flow of steel. J Appl Phys. 1944;15:22–32.
[7] Zhang T, Guo Z-R, Yuan F-P, et al. Investigation on the plastic work-heat conversion coefficient of 7075-T651 aluminum alloy during an impact process based on infrared temperature measurement technology. Acta Mech Sin. 2018;34:327–333.
[8] Rittel D, Zhang LH, Osovski S. The dependence of the Taylor–Quinney coefficient on the dynamic loading mode. J Mech Phys Solids. 2017;107:96–114.
[9] Rittel D, Wang ZG. Thermo-mechanical aspects of adiabatic shear failure of AM50 and Ti6Al4 V alloys. Mech Mater. 2008;40:629–635.
[10] Meyers MA, Subhash G, Kad BK, et al. Evolution of microstructure and shear-band formation in α-hcp titanium. Mech Mater. 1994;17:175–193.
[11] Chichili DR, Ramesh KT, Hemker K J. Adiabatic shear localization in α-titanium: experiments, modeling and microstructural evolution. J Mech Phys Solids. 2004;52:1889–1909.
[12] Rittel D, Landau P, Venkert A. Dynamic recrystallization as a potential cause for adiabatic shear failure. Phys Rev Lett. 2008;101:165501.
[13] Mataya MC, Carr MJ, Krauss G. Flow localization and shear band formation in a precipitation strengthened austenitic stainless steel. MTA. 1982;13:1263–1274.
[14] Meyers MA, Xu YB, Xue Q, et al. Microstructural evolution in adiabatic shear localization in stainless steel. Acta Mater. 2003;51:1307–1325.
[15] Lins JFC, Sandim HRZ, Kestenbach H-J, et al. A microstructural investigation of adiabatic shear bands in an interstitial free steel. Mater Sci Eng: A. 2007;457:205–218.
[16] Meyers MA, Pak H-R. Observation of an adiabatic shear band in titanium by high-voltage transmission electron microscopy. Acta Metall. 1986;34:2493–2499.
[17] Andrade U, Meyers MA, Vecchio KS, et al. Dynamic recrystallization in high-strain, high-strain-rate plastic deformation of copper. Acta Metall Mater. 1994;42:3183–3195.
[18] Nesterenko VF, Meyers MA, LaSalvia JC, et al. Shear localization and recrystallization in high-strain, high-strain-rate deformation of tantalum. Mater Sci Eng: A. 1997;229:23–41.
[19] Murr LE, Niou C-S, Feng C. Residual microstructures in explosively formed tantalum penetrators. Scr Metall Mater. 1994;31:297–302.
[20] Meyers MA, Chen Y-J, Marquis FDS, et al. High-strain, high-strain-rate behavior of tantalum. MMTA. 1995;26:2493–2501.
[21] Nemat-Nasser S, Isaacs JB, Liu M. Microstructure of high-strain, high-strain-rate deformed tantalum. Acta Mater. 1998;46:1307–1325.
[22] Xu YB, Zhong WL, Chen YJ, et al. Shear localization and recrystallization in dynamic deformation of 8090 Al–Li alloy. Mater Sci Eng: A. 2001;299:287–295.
[23] Xu Y, Zhang J, Bai Y, et al. Shear localization in dynamic deformation: microstructural evolution. Metall Mat Trans A. 2008;39:811–843.
[24] Guo Y, Ruan Q, Zhu S, et al. Temperature rise associated with adiabatic shear band: causality clarified. Phys Rev Lett. 2019;122:015503.
[25] Doherty RD, Hughes DA, Humphreys FJ, et al. Current issues in recrystallization: a review. Mater Sci Eng: A. 1997;238:219–274.
[26] Callister WD, Rethwisch DG. Materials science and engineering: an introduction. 8th ed. Hoboken (NJ): Wiley; 2010.

[27] Williams DB, Carter CB. Transmission electron microscopy: a textbook for materials science. 2nd ed. New York: Springer; 2009.
[28] Midgley PA, Eggeman AS. Precession electron diffraction – a topical review. IUCrJ. 2015;2:126–136.
[29] Sagapuram D, Viswanathan K, Mahato A, et al. Geometric flow control of shear bands by suppression of viscous sliding. Proc R Soc A. 2016;472:20160167.
[30] Sagapuram D, Viswanathan K. Evidence for Bingham plastic boundary layers in shear banding of metals. Extreme Mech Lett. 2018;25:27–36.
[31] Viladot D, Véron M, Gemmi M, et al. Orientation and phase mapping in the transmission electron microscope using precession-assisted diffraction spot recognition: state-of-the-art results: REVIEW OF PACOM (ASTAR) APPLICATION. J Microsc. 2013;252:23–34.
[32] Kuhlmann-Wilsdorf D, Hansen N. Geometrically necessary, incidental and subgrain boundaries. Scr Metall Mater. 1991;25:1557–1562.
[33] Tsuji N, Gholizadeh R, Ueji R, et al. Formation mechanism of ultrafine grained microstructures: various possibilities for fabricating bulk nanostructured metals and alloys. Mater Trans. 2019;60:1518–1532.
[34] Wang T, Li B, Wang Z, et al. Formation mechanism of the high-speed deformation characteristic microstructure based on dislocation slipping and twinning in α-titanium. J Mater Res. 2016;31:3907–3918.
[35] Cao Y, Ni S, Liao X, et al. Structural evolutions of metallic materials processed by severe plastic deformation. Mater Sci Eng: R: Rep. 2018;133:1–59.